Dynamics of the Multifragmentation of 1*A* GeV Gold on Carbon

J. A. Hauger,[1] S. Albergo,[2] F. Bieser,[6] F. P. Brady,[3] Z. Caccia,[2] D. A. Cebra,[3] A. D. Chacon,[7] J. L. Chance,[3] Y. Choi,[1,*] S. Costa,[2] J. B. Elliott,[1] M. L. Gilkes,[1,†] A. S. Hirsch,[1] E. L. Hjort,[1] A. Insolia,[2] M. Justice,[5] D. Keane,[5] J. C. Kintner,[3] V. Lindenstruth,[4,‡] M. A. Lisa,[6] U. Lynen,[4] H. S. Matis,[6] M. McMahan,[6] C. McParland,[6] W. F. J. Müller,[4] D. L. Olson,[6] M. D. Partlan,[3,‡] N. T. Porile,[1] R. Potenza,[2] G. Rai,[6] J. Rasmussen,[6] H. G. Ritter,[6] J. Romanski,[2,§] J. L. Romero,[3] G. V. Russo,[2] H. Sann,[4] R. Scharenberg,[1] A. Scott,[5] Y. Shao,[5,‖] B. K. Srivastava,[1] T. J. M. Symons,[6] M. Tincknell,[1] C. Tuvé,[2] S. Wang,[5] P. Warren,[1] H. H. Wieman,[6] T. Wienold,[6] and K. Wolf[7]

(EOS Collaboration)

[1]*Purdue University, West Lafayette, Indiana 47907*
[2]*Universitá di Catania and Istituto Nazionale di Fisica Nucleare-Sezione di Catania, 95129 Catania, Italy*
[3]*University of California, Davis, California 95616*
[4]*GSI, D-64220 Darmstadt, Germany*
[5]*Kent State University, Kent, Ohio 44242*
[6]*Nuclear Science Division, Lawrence Berkeley National Laboratory, Berkeley, California 94720*
[7]*Texas A&M University, College Station, Texas 77843*

(Received 15 March 1996)

An exclusive study of the interaction of 1*A* GeV Au with C shows a separability into two stages: a prompt stage involving emission of most $Z = 1$ and some $Z = 2$ particles and a second stage involving the decay of an equilibrated remnant, which typically undergoes multifragmentation. The mean mass, charge, excitation energy, and the initial temperature T_i of the remnant have been determined as a function of the total charge multiplicity, m, as has the freeze-out temperature T_f. Both T_i and T_f increase linearly with m and their values at the critical point have been determined. T_f rises monotonically with excitation energy as expected for a continuous phase transition. [S0031-9007(96)00615-1]

PACS numbers: 25.75.Dw

We have recently extracted the critical exponents γ, β, τ, and σ from a model independent analysis of the multifragment breakup of 1*A* GeV gold ions incident on carbon [1,2]. The values of these exponents were found to be remarkably close to those for ordinary fluids [3]. These results indicate that multifragmentation (MF) may arise from a continuous phase transition, and may belong to the same universality class as ordinary fluids. They also can provide direct information about the equation of state of nuclear matter in the vicinity of its critical point [4].

The determination of the critical exponents is based on a number of assumptions, the validity of which rests in the MF dynamics. These assumptions are (1) the formation of an equilibrated remnant with charge Z_i, mass A_i, excitation energy E^*, and temperature T_i, following the emission of prompt particles in a first stage and (2) the direct proportionality between the total charged particle multiplicity, m, and temperature [5]. The target independence of MF in heavy ion interactions [6] indicates that the entrance and exit channels are decoupled, consistent with (1). Fragment energy spectra have shown that MF occurs in the breakup of a system lighter than the original nucleus with a strongly reduced Coulomb energy [7–10], suggesting that the remnant undergoes expansion and cooling prior to MF [11] with freeze-out occurring at a temperature T_f. In this Letter we explore the validity of the above assumptions in light of the MF dynamics, determine the above properties of the remnant as a function of m, and determine $T_f(m)$. The values of T_i and T_f at the critical multiplicity, m_c, bracket the critical temperature of the nucleus.

The experimental apparatus, described in detail in [1], consisted of a time projection chamber [12], a time-of-flight wall, and a multiple sampling ionization chamber [13]. These detectors allowed us to identify the nuclear charges and momenta of all charged projectile fragments with high efficiency. Mass identification was possible for $Z \leq 5$. The analysis is based on 33 000 fully reconstructed events, where the total charge for the Au system was found to be 79 ± 3.

Figure 1 shows the laboratory rapidity distributions of several light fragments. In this reverse kinematics experiment, we see that many of the fragments are moving near beam rapidity. This is the case for all Li and higher Z fragments, which show strong peaking near y_{beam}. The symmetry of these distributions is consistent with emission from an equilibrated projectile remnant. In contrast, the lighter particles, particularly p, d, and ^{3}He, show extensive tailing at low y from peaks near y_{beam}. These tails are due to particles which are knocked out of the Au nucleus in the first stage of the interaction.

To determine the mass-weighted average velocity of the projectile remnant we used the Li, Be, and B fragments to compute a mean velocity β_z. We find $\beta_z = 0.873$

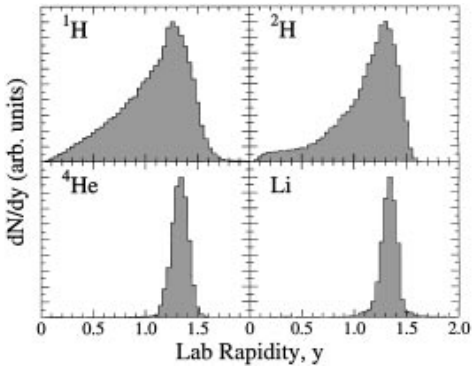

FIG. 1. Laboratory rapidity distributions for light fragments. $y_{\text{beam}} = 1.35$.

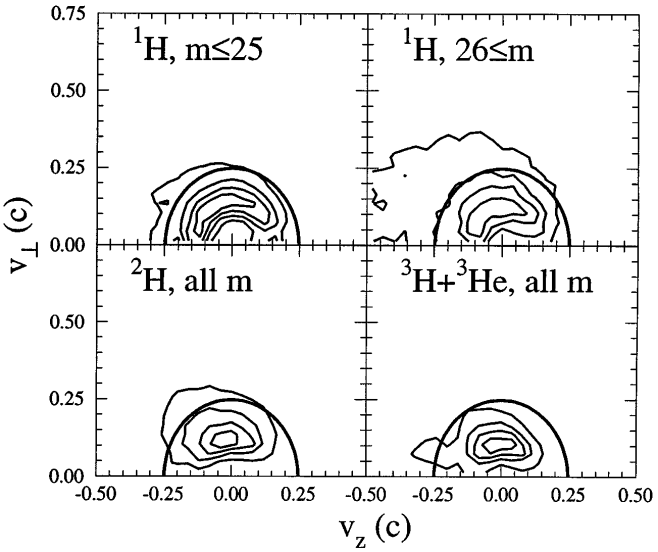

FIG. 2. Contour plot of invariant cross sections for light particle emission in the indicated multiplicity bins. The linear contours correspond to equal particle number intervals. The heavy curves are cuts separating first and second stage particles.

for low m, decreasing monotonically to 0.867 for high m. A linear interpolation gives $\beta_z(m)$. As a check on the accuracy of this velocity we have computed the masses of various heavy fragments using the experimental momenta and $\beta_z(m)$. The mean masses of C, N, and O fragments agree within 1% with the corresponding values obtained from a yield-weighted average of isotopically resolved fragments in high-energy p-Xe interactions [14]. The mean masses of fragments with $Z > 10$ show a similar agreement with values deduced from the EPAX parametrization of the most probable charges of products formed in high-energy reactions [15].

We can examine the behavior of the invariant cross sections as a function of $v_\perp$ and v_z, the transverse and longitudinal velocity components in the moving system. The results for several light particles are shown in Fig. 2. The contours are nearly symmetric about $v_z = 0$ for low $v_\perp$, indicating approximately isotropic emission in the projectile frame. However, for higher $v_\perp$ the contours skew towards negative v_z, as expected for prompt emission. We have made a constant 30 MeV cut in the proton kinetic energies in the moving system in order to separate the two sources in an approximate way. The same energy per nucleon cuts have been made for the other $Z = 1$ and $Z = 2$ particles. The cuts determine particle yields for the two stages. The first stage multiplicity, m_1, consists of ~70% of the $Z = 1$ particles and ~10% of the $Z = 2$ particles. The second stage equilibrium multiplicity, m_2, is linearly proportional to m_1, and $m_2 \simeq \frac{1}{3}m$. By varying the position of the cuts in a manner that preserves approximate isotropy, i.e., between 25 and 35 MeV per nucleon, we estimate a 7% uncertainty in m_2.

We determine Z_i by subtracting from 79 the charges of the prompt $Z = 1$ and $Z = 2$ particles. To obtain A_i we assume the knockout of 1.7 prompt neutrons per prompt proton on the basis of a cascade simulation [16]. Figure 3(a) shows the linear variation of m_2 with m. This linearity is the chief basis of our previous assertion that the inclusion of prompt particles does not significantly change the values of the critical exponents [1,17].

To determine E^*/A_i we use the energy balance relation [18]

$$E^*/A_i = (1/A_i)\left[\sum_j (E_j^{\text{kin}} + Q_j) + 3nT_i/2 + Q_n\right], \tag{1}$$

where E_j^{kin} and Q_j are the kinetic energy in the moving system and the separation energy of the jth charged fragment emitted in the equilibrium stage, respectively, n is the second stage neutron multiplicity, and Q_n is the sum of the separation energy of these neutrons. The mean neutron kinetic energy has been assumed to be $\frac{3}{2}T$, corresponding to volume emission [19]. The value of n, ~10 on average, is the difference between A_i and the sum of the second stage fragment masses. In order to relate E^* and T in Eq. (1) we assume the Fermi gas model relation, $T = (E^*/a)^{1/2}$, where the level density parameter a is taken as $A/13$. This value is consistent with the observed decrease of a with increasing E^* from ~$A/8$ to ~$A/13$, at which point a appears to level off [20]. This fixed value of a is consistent with the range of values of a obtained when T_i is extracted from E^* as a function of m; see below. Equation (1) is quadratic in $(E^*/A)^{1/2}$ and has only one physical solution.

As a test of the procedure embodied in Eq. (1), we have applied it to simulated events generated by the ISABEL cascade code [16] coupled with a statistical MF model (SMM) [21]. The energies of SMM fragments and neutrons lead to E^* values that are in very good agreement with those given for the same events by ISABEL.

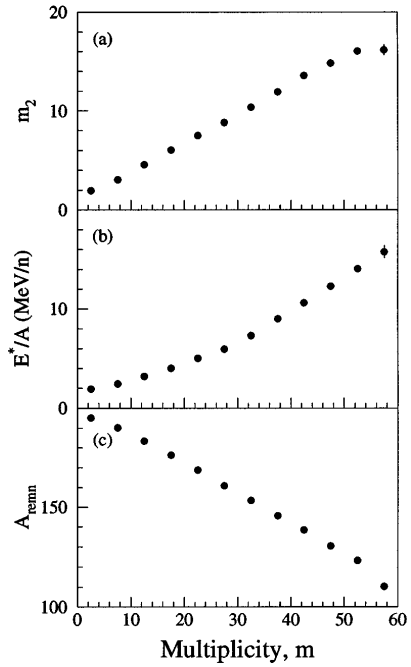

FIG. 3. Dependence on total charge multiplicity of (a) the second stage multiplicity, (b) the mean excitation energy per nucleon of the remnant, and (c) the mean mass of the remnant. Statistical errors are smaller than the size of the points where not shown.

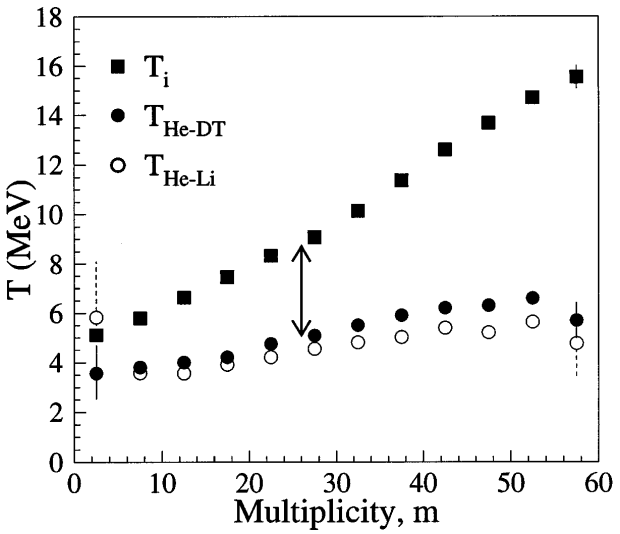

FIG. 4. Variation of T_i and T_f with m. Two different values of T_f are shown, $T_{\text{He-DT}}$ and $T_{\text{He-Li}}$. The double arrow spans the values of the critical temperature.

Figure 3(b) shows the variation of the mean E^*/A_i with m. The result is subject to systematic errors associated with the source velocity determination, mass identification, first stage cut, and neutron number and energy. These effects were investigated by making reasonable changes in the velocity cut and in the assumptions about neutron emission. The combined uncertainty from these sources is $\sim$15%. The nonlinear dependence of E^*/A_i on m reflects the increase of E^* with m and the associated decrease in A_i [Fig. 3(c)]. Thus the mass of the remnant decreases from $\sim$190 to $\sim$110.

The temperature of the unexpanded remnant with mass A_i may be obtained from E^* according to the single component Fermi gas model. It is assumed that the remnant thermalizes in the volume formerly occupied by the Au projectile. Figure 4 shows that T_i is a practically linear function of m in the region where MF occurs, $m \sim 10{-}60$, thereby confirming one of the assumptions in the determination of the critical exponents [1,2]. At the critical multiplicity, $m_c = 26 \pm 1$ [1], $T_i = 8.7 \pm 0.7$ MeV, where the error reflects the uncertainty of the input parameters in the Fermi gas model.

The equilibrated remnant expands and cools prior to breakup. The freeze-out temperature may be obtained from the ratio of isotope yield ratios, where each pair of isotopes differs by one neutron [22]. Pochodzalla *et al.* [23] recently used the ^{3}He/^{4}He and ^{6}Li/^{7}Li yield ratios to determine T_f for the interaction of 600A MeV Au plus Au. We have used this He-Li thermometer as well as a He-DT thermometer based on the ^{2}H/^{3}H yield ratio to estimate T_f. Both T_f were obtained by means of equations given in Ref. [22]. Our results have not been corrected for feed-in from the decay of heavier fragments, which has been estimated as a 20% correction [23]. We believe that the $T_{\text{He-DT}}$ are more accurate than the $T_{\text{He-Li}}$ because they do not require a correction for low-lying excited states. In addition to the statistical error, the error in $T_{\text{He-DT}}$ is due to the uncertainty in the separation between the first and second stages, which is $\sim$3%.

Figure 4 shows the variation of T_f with m. Both thermometers give similar results and indicate that T_f is a linear function of m. When $m = m_c$, $T_f = 5.1 \pm 0.2$ MeV. This temperature is close to the cracking temperature predicted by various statistical models [21,24] and also agrees with a determination based on a thermal liquid drop model description of the isotopic yields of fragments from p-Xe collisions [8]. Figure 4 shows that $T_{\text{He-DT}}$ is substantially lower than T_i, where their ratio decreases from 0.77 for low m to 0.51 for high m. Evidently, the remnant cools down on its approach to freeze-out due to both expansion and evaporation, with a higher degree of cooling occurring at high E^*. The values of $T_f(m_c)$ and $T_i(m_c)$ bracket the critical temperature of the nucleus, which thus has a value between $\sim$5 and 9 MeV.

Figure 5 shows the monotonic increase of $T_{\text{He-DT}}$ with E^*/A_i. This variation is consistent with that expected for a liquid-gas phase transition in the critical region. Pochodzalla *et al.* [23] have presented a similar curve for the interaction of 600A MeV Au with Au which displays a roughly constant value of $T_{\text{He-Li}}$ between 2 and 10 MeV/nucleon followed by a sharp rise at higher E^*/A_i. At the highest E^*/A_i, where the difference in the

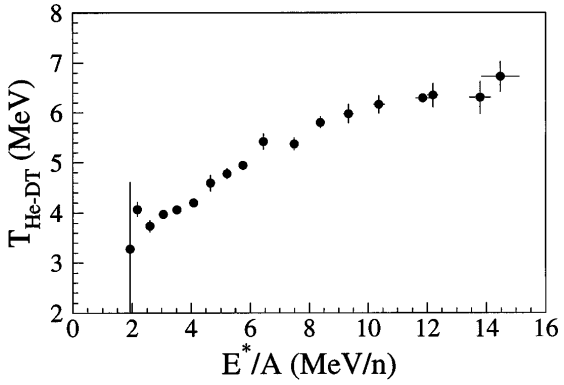

FIG. 5. Dependence of $T_{\text{He-DT}}$ on E^*/A_i. Statistical errors are smaller than the size of the points where not shown.

shape of the two curves is largest, their remnant masses are only half as large as ours. Consequently, the two systems may differ in dynamics. A detailed comparison is presented elsewhere [25].

In summary, we have separated the first stage particles from those emitted by an equilibrated remnant in the interaction of 1A GeV ^{197}Au with carbon. Most of the $Z = 1$ particles as well as a small fraction of the $Z = 2$ particles are emitted prior to equilibrium. Heavier fragments are emitted by the equilibrated remnant, the charge and mass of which have been determined as a function of m. The second stage multiplicity is a linear function of m, where $m_2 \simeq \frac{1}{3}m$. The mean excitation energy of the remnant has been determined and the temperature T_i derived from it is a linear function of m. These results validate the assumptions made in our previous determination of the critical exponents. The freeze-out temperature T_f has been determined using two different isotope ratio thermometers and is also a linear function of m. The values of $T_i(m_c)$ and $T_f(m_c)$ bracket the critical temperature of the nucleus. The monotonic increase of $T_{\text{He-DT}}$ with E^*/A_i supports the view that MF may indeed result from a continuous phase transition near the critical point.

This work was supported in part by the U.S. Department of Energy under Contracts or Grants No. DE-ACO3-76SF00098, No. DE-FG02-89ER40531, No. DE-FG02-88ER40408, No. DE-FG02-88ER40412, No. DE-FG05-88ER40437, and by the U.S. National Science Foundation under Grant No. PHY-91-23301.

*Present address: Sung Kwun Kwan University, Suwon 440746, Republic of Korea.
†Present address: State University of New York, Stony Brook, NY 11790.
‡Present address: Nuclear Science Division, Lawrence Berkeley National Laboratory, Berkeley, CA 94720.
‡
§The Svedberg Laboratory, University of Uppsala, S751-21 Uppsala, Sweden.
‖Present address: Crump Institute for Biological Imaging, UCLA, Los Angeles, CA 91776.

[1] M. L. Gilkes *et al.*, Phys. Rev. Lett. **73**, 1590 (1994).
[2] J. B. Elliott *et al.*, Phys. Lett. B (to be published).
[3] H. E. Stanley, *Introduction to Phase Transitions and Critical Phenomena* (Oxford University Press, Oxford, 1971).
[4] K. C. Chase and A. Z. Mekjian, Phys. Rev. Lett. **75**, 4732 (1995).
[5] X. Campi, J. Phys. A **19**, L917 (1986); Phys. Lett. B **208**, 351 (1988); in *Proceedings of the International School of Physics "Enrico Fermi"* (North-Holland, Amsterdam, 1990), p. 237.
[6] J. Hubele *et al.*, Phys. Rev. C **46**, R1577 (1992).
[7] A. M. Poskanzer *et al.*, Phys. Rev. C **3**, 882 (1971).
[8] A. S. Hirsch *et al.*, Phys. Rev. C **29**, 508 (1984).
[9] N. T. Porile *et al.*, Phys. Rev. C **39**, 1914 (1989).
[10] K. Kwiatkowski *et al.*, Phys. Rev. Lett. **74**, 3756 (1995).
[11] W. A. Friedman, Phys. Rev. C **42**, 667 (1990).
[12] G. Rai *et al.*, IEEE Trans. Nucl. Sci. **37**, 56 (1990).
[13] W. Christie *et al.*, Nucl. Instrum. Methods Phys. Res., Sect. A **255**, 46 (1987).
[14] R. W. Minich *et al.*, Phys. Lett. B **118**, 458 (1982).
[15] K. Sümmerer *et al.*, Phys. Rev. C **42**, 2546 (1990).
[16] Y. Yariv and Z. Fraenkel, Phys. Rev. C **20**, 2227 (1979).
[17] M. Gilkes *et al.*, Phys. Rev. Lett. **75**, 768 (1995).
[18] D. Cussol *et al.*, Nucl. Phys. **A561**, 298 (1993).
[19] R. Wada *et al.*, Phys. Rev. C **39**, 497 (1989).
[20] K. Hagel *et al.*, Nucl. Phys. **A486**, 429 (1988).
[21] J. P. Bondorf *et al.*, Phys. Rep. **257**, 133 (1995).
[22] S. Albergo *et al.*, Nuovo Cimento So. Ital. Fis. **89A**, 1 (1985).
[23] J. Pochodzalla *et al.*, Phys. Rev. Lett. **75**, 1040 (1995).
[24] D. H. E. Gross, Rep. Prog. Phys. **53**, 605 (1990).
[25] M. Tincknell *et al.*, Proceedings of the 12th Winter Workshops on Nuclear Dynamics (to be published).